Transport of Heat, CO$_{2}$ and O$_{2}$ by the Atlantic's Thermohaline Circulation

Ralph F. Keeling and Tsung-Hung Peng

Email alerting service	Receive free email alerts when new articles cite this article - sign up in the box at the top right-hand corner of the article or click **here**

Transport of heat, CO_2 and O_2 by the Atlantic's thermohaline circulation

RALPH F. KEELING[1] AND TSUNG-HUNG PENG[2]

[1] *Scripps Institution of Oceanography, La Jolla, California 92093–0236, U.S.A.*
[2] *Ocean Chemistry Division, NOAA/AOML/OCD, 4301 Rickenbacker Causeway, Miami, Florida 33149 U.S.A.*

SUMMARY

We estimate transport of heat, CO_2 and O_2 by the Atlantic's thermohaline circulation using an approach based on differences in the chemical and physical characteristics of North Atlantic Deep Water (NADW), Antarctic Intermediate Water (AAIW), and the northward return flow across the equator. The characteristics of the return-flow waters are constrained by imposing conservation of phosphate in the North Atlantic as a whole. Based on a total equatorial return flow of 13×10^6 m^3 s^{-1}, we find that the Atlantic north of the equator is a source of $7.7 \pm 1.4 \times 10^{14}$ W to the atmosphere, a sink of $0.51 \pm 0.21 \times 10^{14}$ mol of O_2, and preindustrially was a sink of $0.33 \pm 0.15 \times 10^{14}$ mol of CO_2. Uptake of O_2 and CO_2 by the North Atlantic is driven mainly by thermal, as opposed to biological processes.

1. INTRODUCTION

The North Atlantic is unique among the world's oceans in that its surface water is believed to be exchanged with the other oceans by thermohaline circulation rather than by wind-driven transport. Surface water leaves the North Atlantic by flowing northward into the Labrador, Greenland, and Norwegian Seas where it cools sufficiently to sink to great depths. These newly formed deep waters intermix in the deep Labrador Sea to form a water mass known as the North Atlantic Deep Water (NADW) which is transported by a system of deep currents along the western boundary of the North Atlantic across the equator and into the southern ocean (see, for example, Schmitz & McCartney 1993).

The return flow needed to balance the exported NADW originates, according to Schmitz & McCartney (1993), as Antarctic Intermediate Water (AAIW) that is warmed by upwelling in the South Atlantic and along the equator so that it enters the North Atlantic within the thermocline or at the surface. Important questions remain, however, over the origin and pathways of the return flow (Gordon 1985; Rintoul 1991; Schmitz & Richardson 1991).

The Atlantic's thermohaline circulation, sometimes known as the conveyor circulation (Broecker 1991), contributes to a net northward transport of heat because the northward flowing waters are warmer than the southward flowing deep waters. The conveyor circulation also leads to a net southward transport of both CO_2 and O_2 through the ocean (Brewer *et al.* 1989; Rintoul & Wunsch 1991; Broecker & Peng 1992).

Our principal purpose here is to re-examine inter-hemispheric transport of O_2 and CO_2 caused by the conveyor circulation, as a precursor to interpreting observations of atmospheric O_2 and CO_2 (see, for example, Keeling & Shertz 1992). The fluxes of O_2 and CO_2 carried by the oceans must be balanced, assuming a steady state, by reverse fluxes through the atmosphere. These atmospheric fluxes of oceanic origin are superimposed on additional O_2 and CO_2 fluxes driven by exchanges with terrestrial ecosystems and by fossil-fuel burning. A better understanding of the oceanic contribution to these fluxes is needed, for example, in order to apply atmospheric O_2 and CO_2 data to constrain CO_2 exchanges with terrestrial ecosystems (Keeling *et al.* 1989, 1993; Tans *et al.* 1990).

The approach we have taken to compute inter-hemispheric O_2 and CO_2 fluxes is essentially an extension of the method used by Broecker & Peng (1992) for computing CO_2 fluxes. The approach allows us to obtain first-order estimates of the fluxes across the equator where direct calculations based on geostrophic and Eckman transports (e.g. Hall & Bryden 1982; Rintoul & Wunsch 1991) face difficulties. We are interested in the fluxes across the Equator because the observable interhemispheric gradients in atmospheric CO_2 and O_2 are mainly dependent on transport across the tropics where the barrier to north–south atmospheric mixing is greatest. Because the application is straightforward, we also apply the method to compute transports of heat which are relevant to climate and climate modelling studies (e.g. Broecker 1991; Isemer *et al.* 1989).

The method used here involves examining the properties of three water masses along the conveyor's path: first, in newly forming NADW, second in AAIW, and third in the water returning northward across the equator. Air–sea fluxes are computed by simply multiplying the water flux by the difference of the
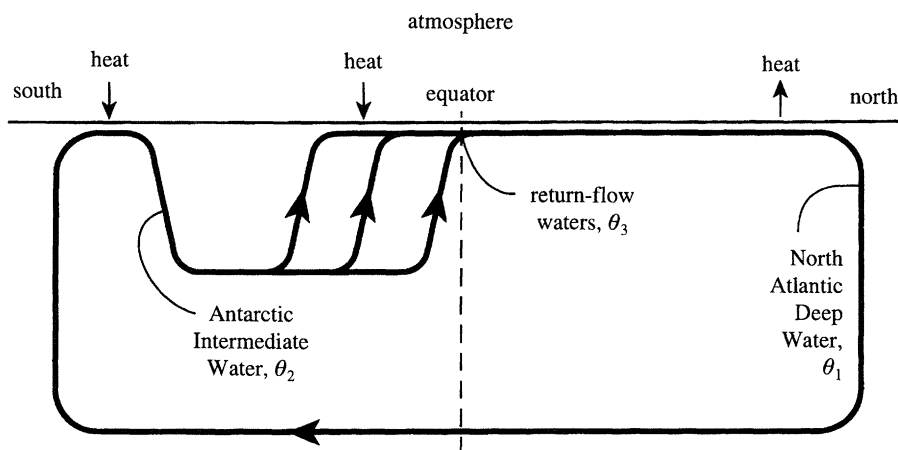
133

Figure 1. Illustrating the approach used to estimate heat transport by conveyor circulation. θ_1, θ_2, and θ_3 represent the average potential temperatures of North Atlantic Deep Water, Antarctic Intermediate Water, and waters returning northward across the equator, respectively. Conversion from one water mass to the next along the conveyor requires heat exchanges with the atmosphere that can be directly calculated from the differences in the potential temperatures of the water masses and the total volume flow rate of the conveyor circulation.

properties in the three water masses. The method, as applied to compute transports of heat, is illustrated in figure 1. In principle, the method can be applied to compute transports of any tracer that is conservative in the sense that its concentration in a water parcel can only be changed by exchanges with the atmosphere.

2. TRACERS FOR CO_2 AND O_2 TRANSPORT

To apply the approach to compute fluxes of CO_2 and O_2 we need to find conservative tracers in the ocean that keep track of the exchanges of these gases with the air. Total dissolved CO_2 (ΣCO_2) and dissolved O_2 are not conservative: both are altered within a water mass by photosynthesis and respiration, and ΣCO_2 is additionally altered by the dissolution and precipitation of calcium carbonate. To correct for these alterations we follow Broecker & Peng (1992) by using dissolved phosphate to measure the extent of photosynthesis versus respiration and by using the nitrate-corrected alkalinity to measure the extent of dissolution of calcium carbonate. They define the following tracers

$$\Delta \Sigma CO_2 = \Sigma CO_2 - 1900 \times \frac{S}{35} - 127\,PO_4$$

$$-\frac{1}{2}\left(Alk + NO_3 - 2310 \times \frac{S}{35}\right),$$

and

$$PO_4{}^* = PO_4 - 1.95 + \frac{O_2}{175},$$

where S is the salinity, Alk is the alkalinity, and where factors of 127 and 175 represent the global average 'Redfield' ratio of O_2 consumption and CO_2 release to phosphate release during respiration (Takahashi *et al.* 1985; Peng & Broecker 1987). To the extent that these factors are constant throughout the ocean, the tracers $\Delta \Sigma CO_2$ and $PO_4{}^*$ are conservative. The expression for $\Delta \Sigma CO_2$ includes salinity corrections to total dissolved

CO_2 and alkalinity to account for changes caused simply by addition or removal of fresh water. The constant term (1.95) is arbitrary. Changes in $\Delta \Sigma CO_2$ and $175 \times PO_4{}^*$ effectively measure the integrated amount of atmospheric CO_2 and O_2, respectively, which a water parcel has taken up or released, and they are thus the conservative analogues of atmospheric CO_2 and O_2 that we need for our transport calculations.

In the case of O_2 it is possible to divide the air–sea fluxes computed based on $PO_4{}^*$ into separate 'thermal' and 'biological' components. This is because, in the absence of biological activity, O_2 would tend to remain close to equilibrium with the atmosphere. We can, therefore, approximate the 'thermal' transport as being simply proportional to O_2 solubility. It follows that the remaining 'biological' transport is proportional to the flux of preformed phosphate (Redfield *et al.* 1963), another conservative tracer, defined here by

$$PO_4{}^{(pref)} = PO_4 - AOU/175,$$

where AOU is the apparent oxygen utilization. The thermal O_2 fluxes computed from O_2 solubility are slight overestimates of the true thermal O_2 fluxes because a water parcel that fully equilibrates with the atmosphere on warming or cooling exchanges more O_2 with the air than a water parcel that does not fully equilibrate (see also Keeling *et al.* 1993).

Special consideration is needed to estimate CO_2 exchanges because the ocean carbon cycle is currently not in a steady state as a result of the build-up of anthropogenic CO_2 in the atmosphere and its redistribution into the ocean. Our interest here, however, is limited to estimating the fluxes that existed prior to the anthropogenic perturbation, and following Broecker & Peng (1993), we estimate these exchanges by correcting the observed $\Delta \Sigma CO_2$ values back to their preanthropogenic values.

3. FLUX CALCULATIONS

The first step for computing the air–sea exchanges of heat, CO_2, total O_2 and 'biological O_2' is to determine the average values of potential temperature θ, $\Delta\Sigma CO_2$, PO_4*, and $PO_4^{(pref)}$ in the three water masses: NADW, AAIW, and the return-flow waters. For NADW and AAIW this task is relatively straightforward because these water masses are relatively homogenous in these tracers, as shown in figures 2 and 3.

Defining the average characteristics of the return-flow waters presents a more serious challenge. From general considerations we know that the waters contributing to the return flow have potential temperatures greater than about 5 °C. This alone is not very helpful, however, because low-latitude waters warmer than 5 °C exhibit considerable variability in θ, $\Delta\Sigma CO_2$, PO_4*, and $PO_4^{(pref)}$, as shown in figure 4. Fortunately we can limit the range of water characteristics by requiring the fluxes of phosphate carried into or out of the North Atlantic by the ocean currents to sum to zero. This is justified because input of phosphate from rivers and export to sediments is only a tiny fraction of

the flux of phosphate that is carried north and south by the conveyor circulation (Meybeck 1982; Broecker & Peng 1982, pp. 346).

The phosphate concentration in newly formed NADW is around 1.07 μmol kg^{-1}, as can be seen from figure 2 a, so we require an average of 1.07 μmol kg^{-1} of phosphate in the return-flow waters to balance this export. Additionally, we must allow for phosphate that accumulates in the southward flowing NADW plume because of *in situ* remineralization. Using PO_4* to distinguish waters of northern and southern origin, Broecker *et al.* (1991) have estimated oxygen deficiencies from *in situ* respiration in waters deeper than 2000 m in the Atlantic. In the equatorial region, their estimated oxygen utilization varies between 20–30 μmol kg^{-1}. Converting the oxygen utilization to units of phosphate by dividing by 175, we estimate that about 0.14 μmol kg^{-1} of phosphate is added by remineralization to the southward flowing NADW by the time it crosses the equator. Thus we require approximately 1.21 μmol kg^{-1} of phosphate in the return flow to balance the phosphate in newly forming NADW plus that added by remineralization.
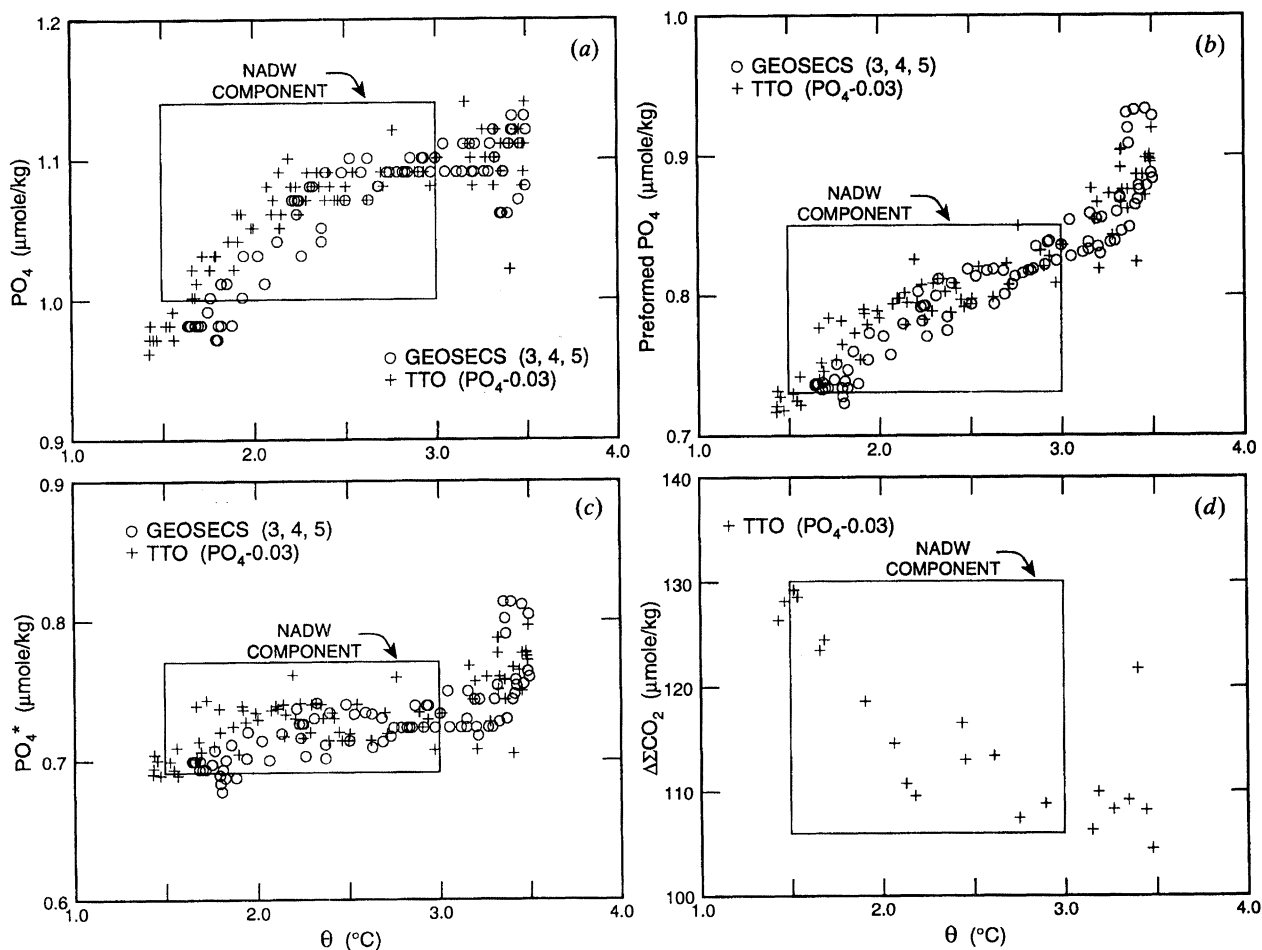

Figure 2. Results from GEOSECS (Bainbridge, 1981) and TTO expeditions (Scripps Institution of Oceanography, 1986) for stations in the deep Labrador Sea with potential temperatures less than 3.5 °C. (a) phosphate versus θ, (b) preformed PO_4 versus θ, (c) PO_4* versus θ, (d) $\Delta\Sigma CO_2$ versus θ. The ranges adopted for the NADW component of θ, PO_4*, preformed PO_4, and $\Delta\Sigma CO_2$ concentrations are indicated. For $\Delta\Sigma CO_2$, a northern component of 105 ± 15 μmol kg^{-1} was taken from Broecker and Peng (1992). The data in the figure indicate that $\Delta\Sigma CO_2$ concentrations in the deep Labrador sea in the early 1980s were somewhat higher than this, presumably as the result of input of anthropogenic CO_2. Following Broecker *et al.* (1991), we have decreased the TTO phosphate for these stations by 0.03 μmol kg^{-1}, to bring the data into better agreement with the GEOSECS data.
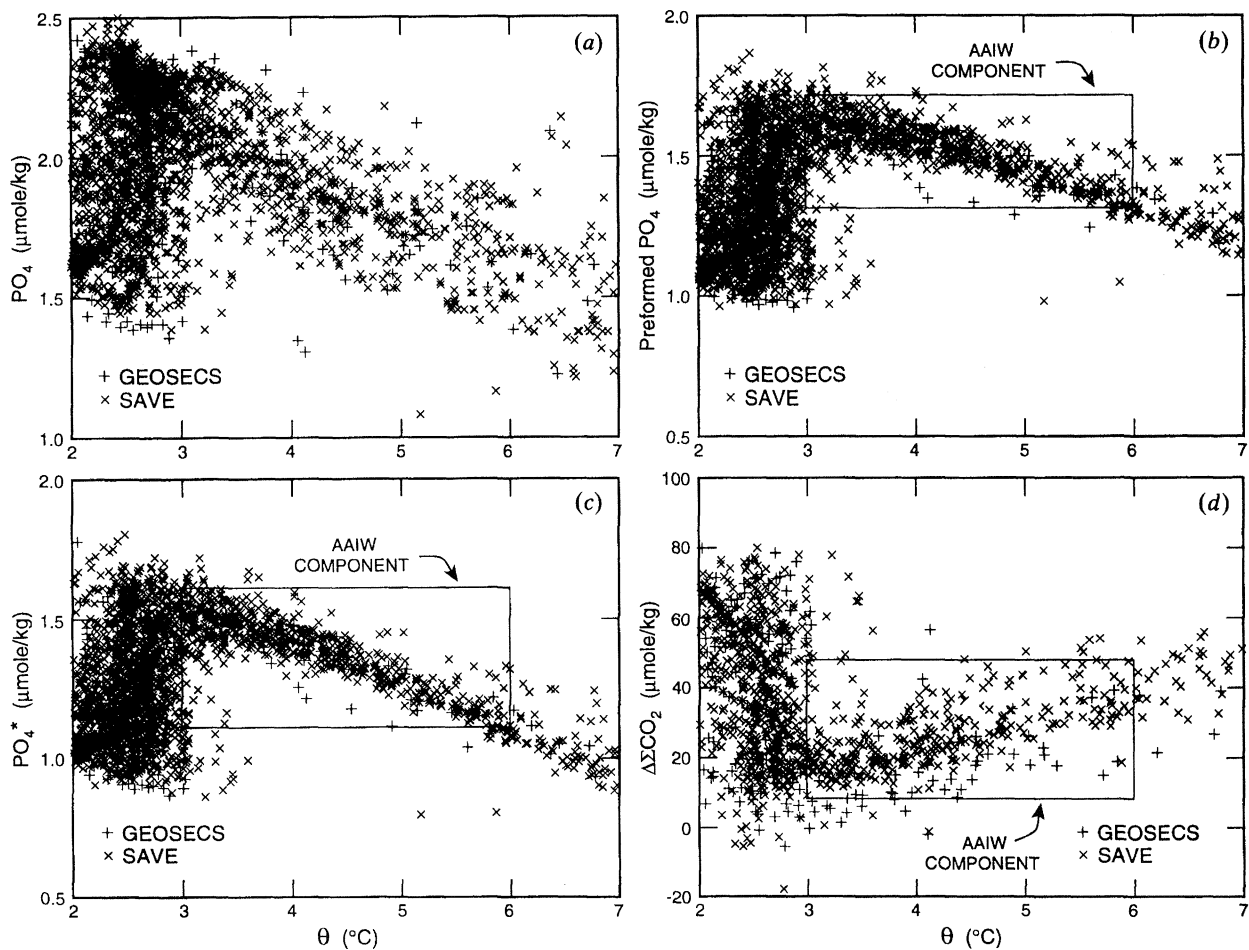
Figure 3. Results from GEOSECS, TTO/TAS, and SAVE (Scripps Institution of Oceanography, 1988) expeditions for Atlantic stations between 30–50 °S. (*a*) phosphate versus θ, (*b*) preformed PO_4 versus θ, (*c*) PO_4* versus θ, (*d*) $\Delta\Sigma CO_2$ versus θ. The ranges adopted for the Antarctic Intermediate Water component are indicated. The anthropogenic correction to $\Delta\Sigma CO_2$ is assumed negligible.

Additionally, we need to allow for phosphate exported from the North Atlantic by sinking organic matter that is remineralized in Antarctic Bottom Water (AABW) that recirculates into and out of the North Atlantic without ever being exposed to the surface. The maps of Broecker *et al.* (1991) indicate that between 10–20 % of the water below 2000 m in the North Atlantic is derived from AABW. Because we do not expect large differences in the rate of respiration in AABW compared to NADW, we can account for phosphate added to recirculating AABW by increasing the respiratory phosphate added to NADW by 15 ± 5 %. Overall, this raises the required phosphate content of the return flow to 1.23 μmol kg^{-1}.

Around 0.8 *Sv* (1 *Sv* = 10^6 m^3 s^{-1}) of the return flow enters the Atlantic from the North Pacific through the Bering Strait and the Arctic Ocean (Coachman & Aagaard 1988). Although the flow is small, the nutrient content of this water is potentially quite high (Björk 1990). To allow for this phosphate contribution to NADW, we assume that the phosphate content of the water passing through the Bering Strait is 2.1 μmol kg^{-1} (Codispoti & Owens 1975), we assume no phosphate is gained or lost in the Arctic Ocean, and we assume that 6 % of the return flow arrives via the arctic route. This figure of 6 % is based on taking 13 *Sv* for the return flow entering the North Atlantic via the

equatorial route (see below). In order to bring the average phosphate content of the combined equatorial and arctic return flows to the required 1.23 μmol kg^{-1}, we need, under these assumptions, an average phosphate content in the equatorial return flow of 1.18 μmol kg^{-1}. We expect this estimate is reliable to within about ± 0.13 μmol kg^{-1}, as we have assumed rather pessimistically that the error contributions from the phosphate content of newly formed NADW (± 0.07), the phosphate added by deep respiration (± 0.04), and the phosphate content of Bering Straits overflow (± 0.4) might be added systematically.

In addition to this phosphate constraint, we impose a second constraint that is based on the argument of Schmitz & McCartney (1993) that waters with potential temperatures between 12–24 °C are effectively blocked from crossing the equator by the equatorial countercurrent. Figure 5*a* indicates that there is a relatively consistent relationship between potential temperature and phosphate over the full range from 5–30 °C, so an equivalent statement is that the waters with phosphate concentrations between about 0.3 and 1.6 μmol kg^{-1} are effectively blocked from crossing the equator. This constraint, plus the relatively consistent relationship between phosphate and θ, PO_4*, $PO_4^{(pref)}$, $\Delta\Sigma CO_2$ as shown in figure 5, suggests that it may be possible to characterize the
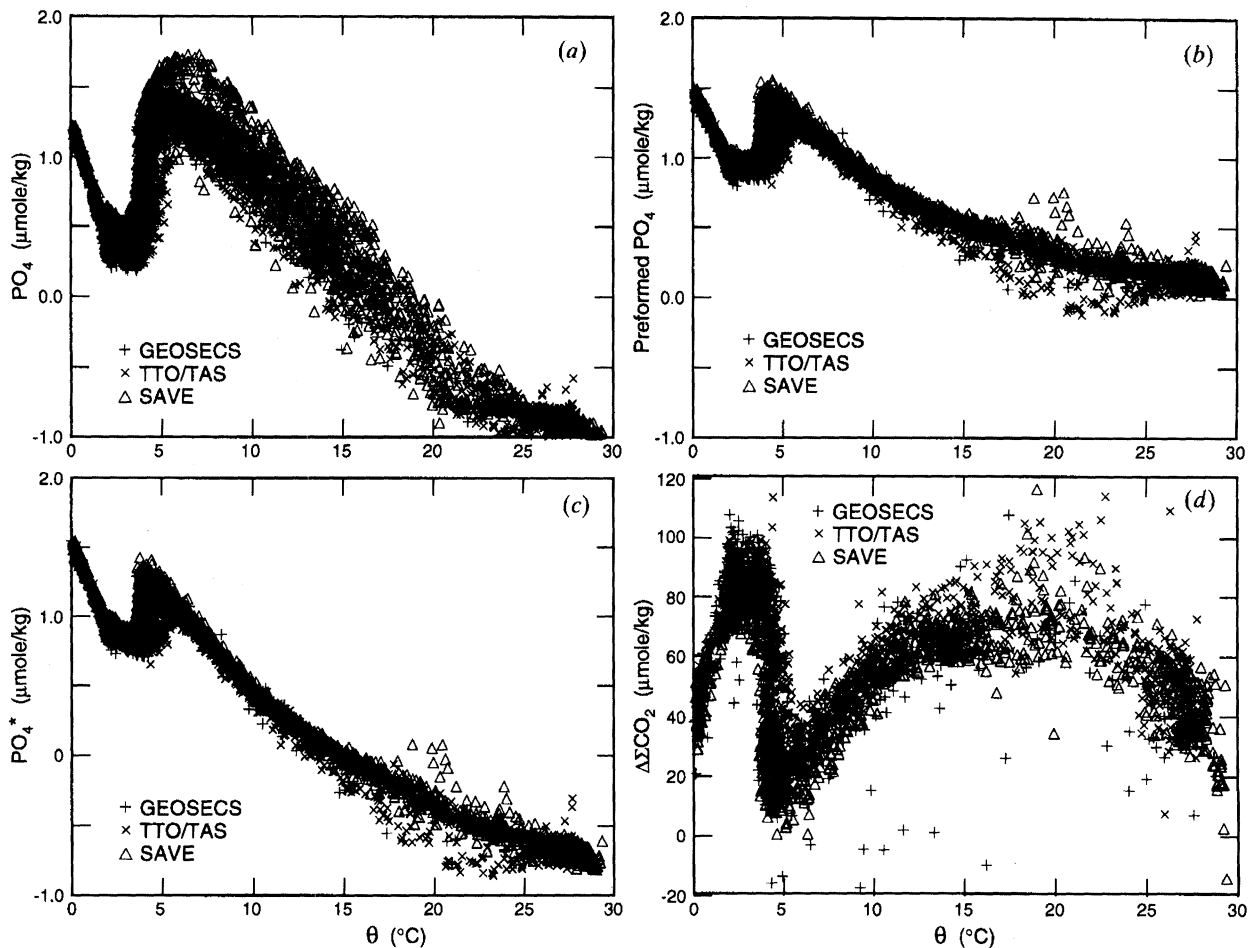
Figure 4. Results from GEOSECS, TTO/TAS and SAVE expeditions for stations between 15 °S and 15 °N. (a) PO_4 versus θ; (b) preformed PO_4 versus θ; (c) PO_4^* versus θ; (d) $\Delta\Sigma CO_2$ versus θ.

average composition of the return flow on the basis of the relative amounts of three endmember components: surface water, lower thermocline water, and intermediate water, with phosphate concentrations of 0.0, 1.7 and 2.4 $\mu mol\ kg^{-1}$, respectively. The approximate chemical composition of these endmembers and their uncertainties are summarized in table 1.

We would like to be able to uniquely determine the relative contributions of each of the three endmembers to the total return flow. This is not possible in the present circumstances because we have only two constraints – the constraint on the total northward flow and the constraint on the average phosphate concentration – but three unknowns. We have chosen to allow for the uncontrolled degree of freedom by considering scenarios in which the return flow consists of two endmembers only. There are only two possible scenarios of this sort, the first in which the return flow consists of just 'surface' and 'lower thermocline' endmembers, and the second in which the return flow consists of just 'surface' and 'intermediate' endmembers. The third scenario with just 'lower thermocline' and 'intermediate' endmembers is ruled out by the phosphate constraint. In the two allowable scenarios, we adjust the proportions of the two endmembers to obtain the required average phosphate concentration of $1.18 \pm 0.13\ \mu mol\ kg^{-1}$. These two scenarios are extreme cases which must bracket the actual budget for the return-flow waters.

The air–sea fluxes involved in converting the return-flow waters to NADW computed for these two 'extreme' scenarios are summarized in table 2. The fluxes are directly proportional to the equatorial return flow for which we adopt a value from Schmitz & McCartney (1993) of 13 *Sv*. The uncertainties allow for variability in the composition of NADW, AAIW, and in the equatorial return-flow water as reflected in uncertainty in the equatorial endmembers and the phosphate constraint. We have made no allowance for uncertainty in the conveyor flow, although recent estimates range as high as 20 *Sv* (Broecker *et al.* 1991). Table 2 also includes a 'composite' scenario calculated by averaging the fluxes for the 'extreme' scenarios. The uncertainty allowed for in the 'composite' scenario includes the full ranges spanned by the two 'extreme' scenarios.

The air–sea fluxes involved in converting NADW to AAIW and in converting AAIW to return-flow waters are summarized in table 3, where the composition of the return-flow waters is taken from the 'composite' scenario. The pattern of heat, O_2, and CO_2 exchange indicated by the composite scenario is shown in figure 6.
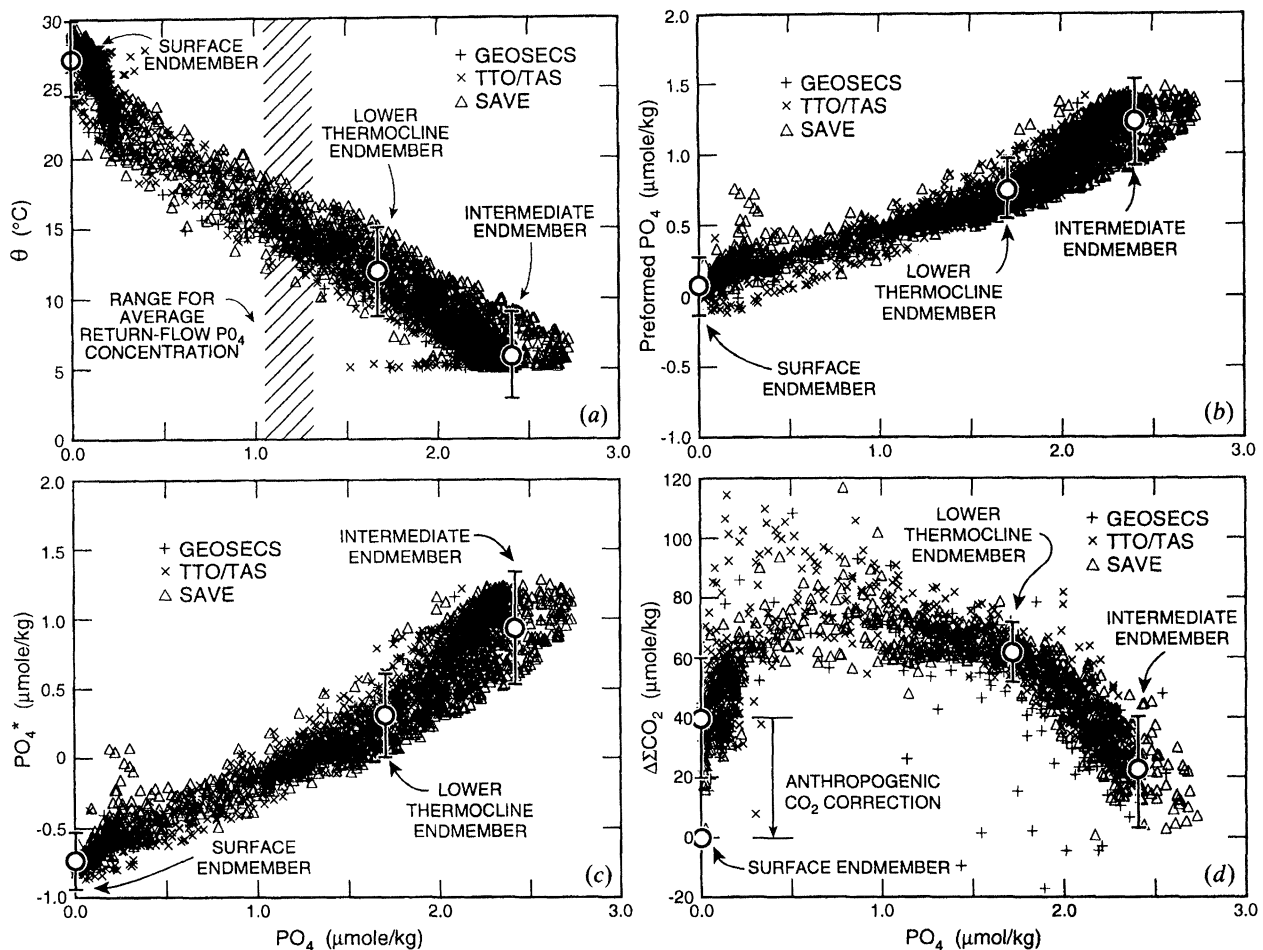
Figure 5. Results from the GEOSECS, TTO/TAS and SAVE expeditions for stations between 15 °S and 15 °N, for $\theta > 5$ °C; (a) θ versus PO_4; (b) preformed PO_4 versus PO_4; (c) $PO_4{}^*$ versus PO_4; (d) $\Delta\Sigma CO_2$ versus PO_4. Average concentrations and uncertainties adopted for the various 'endmembers' are indicated. For the surface endmember we take $\Delta\Sigma CO_2$ from Figure 5 of Broecker & Peng (1993), rather than from this graph. Doing this is consistent with an average anthropogenic correction to the surface waters of around 40 μmol kg^{-1}, as indicated. The anthropogenic CO_2 correction to the other endmembers is assumed to be negligible.

Table 1. *Water mass properties*

| water mass | NADW | AAIW | return flow endmembers | | |
			surface	thermocline	intermediate
potential temperature/°C	2.25 (±0.75)	4.5 (±1.5)	27 (±3)	12 (±3)	6 (±3)
$PO_4/(\mu\text{mol kg}^{-1})$	1.07 (±0.07)		0.0	1.70	2.40
$PO_4{}^{(\text{pref})}/(\mu\text{mol kg}^{-1})$	0.79 (±0.06)	1.51 (±0.2)	0.08 (±0.20)	0.75 (±0.20)	1.22 (±0.30)
$PO_4{}^*/(\mu\text{mol kg}^{-1})$	0.73 (±0.04)	1.36 (±0.25)	-0.73 (±0.20)	0.30 (±0.30)	0.93 (±0.40)
$\Delta\Sigma CO_2/(\mu\text{mol kg}^{-1})$	105 (±12)	28 (±20)	0 (±20)	62 (±10)	22 (±20)

4. DISCUSSION

So far we have been rather vague about what regions of the sea surface correspond to these surface fluxes. In table 3 and figure 6 we have assigned the fluxes associated with converting NADW to AAIW to the Antarctic Ocean because this is where the most vigorous upwelling of deep water takes place, although, we note that some upwelling also occurs in the Pacific and Indian oceans, so this assignment is only ap-

proximate. Following Schmitz and McCartney (1993), we have assigned the fluxes associated with converting AAIW into return-flow waters to the Southern and Equatorial Atlantic. Not only are these regional assignments very approximate, but the computed exchanges include only a portion of the total air–sea exchange that takes place in these southern regions because additional exchanges related to wind-driven transport have been neglected. These difficulties are not of great concern here because our purpose in

Table 2. *Results for North Atlantic fluxes*

	'thermocline' scenario	'intermediate water' scenario	composite scenario
volume transports of return-flow endmembers[a]			
surface water	4.0 ± 1.0	6.6 ± 0.7	3.0 to 7.3
lower thermocline	9.0 ± 1.0	0	0 to 10.0
intermediate Water	0	6.4 ± 0.7	0 to 7.1
average return-flow characteristics[b]			
pot. temp./°C	16.6 ± 3.2	16.7 ± 3.2	16.6 ± 3.3
pref. $PO_4/(\mu mol\ kg^{-1})$	0.54 ± 0.21	0.64 ± 0.26	0.60 ± 0.28
$PO_4^*/(\mu mol\ kg^{-1})$	-0.02 ± 0.30	0.09 ± 0.33	0.04 ± 0.36
$\Delta\Sigma CO_2/(\mu mol\ kg^{-1})$	43 ± 13	11 ± 20	26 ± 33
North Atlantic fluxes[b,c]			
heat flux[d]	7.7 ± 1.4	7.7 ± 1.3	7.7 ± 1.4
bio. O_2 flux[e]	-0.18 ± 0.13	-0.11 ± 0.15	-0.15 ± 0.17
thermal O_2 flux[f]	-0.37 ± 0.07	-0.36 ± 0.07	-0.37 ± 0.07
total O_2 flux[g]	-0.55 ± 0.17	-0.48 ± 0.18	-0.51 ± 0.21
CO_2 flux[h]	-0.26 ± 0.08	-0.40 ± 0.09	-0.33 ± 0.15

[a] Flows are in units of 10^6 m^3 s^{-1}. The uncertainty bounds are set by the constraint that the average phosphate of the return flow must lie in the range of 1.05 and 1.31 $\mu mol\ kg^{-1}$ (see text).

[b] The errors for the 'thermocline' and 'intermediate water' scenarios represent the quadrature sum of errors arising from uncertainties in 'endmember' composition (from table 1) combined with the errors that arise from letting the flows vary within the bounds set by the phosphate constraint. Errors for the composite scenario include the full error ranges spanned by the 'thermocline' and 'intermediate water' scenarios.

[c] Units: heat flux, 10^{14} W; gas fluxes, 10^{14} mols a^{-1}. Fluxes are positive into the atmosphere.

[d] The heat flux is computed according to $Q = \overline{\rho c_p}\Sigma_i\ (\theta_i - \theta_{NADW})\ F_i$, where $\overline{\rho c_p}$ is the heat capacity per unit volume, for which we use a constant value of 4.12×10^6 J m^{-3} K^{-1}, where θ_i and θ_{NADW} are the potential temperature of the return-flow endmember i and NADW, respectively, and where F_i is volume transport of return-flow endmember i.

[e] Computed from $175\overline{\rho}\Sigma_i\ ([PO_4^{pref}]_i - [PO_4^{pref}]_{NADW})\ F_i$ where $\overline{\rho}$ is an appropriate average density, for which we use a value of 1.025×10^3 kg m^{-3}.

[f] Computed from the difference in the biological O_2 flux and the total O_2 flux. The percent uncertainty in the thermal O_2 flux was assumed to be the same as the percentage uncertainty in the heat flux.

[g] Computed from $175\overline{\rho}\Sigma_i\ ([PO_4^*]_i - [PO_4^*]_{NADW})\ F_i$.

[h] Computed from $\overline{\rho}\Sigma_i\ ([\Delta\Sigma CO_2]_i - [\Delta\Sigma CO_2]_{NADW})\ F_i$.

Table 3. *Results for Southern Hemisphere fluxes*[a]

	Antarctic Ocean fluxes	Southern and Equatorial Atlantic fluxes
heat flux	-1.2 ± 0.9	-6.5 ± 1.6
bio. O_2 flux	-0.53 ± 0.15	0.68 ± 0.23
thermal O_2 flux	0.07 ± 0.05	0.30 ± 0.07
total O_2 flux	-0.47 ± 0.19	0.98 ± 0.29
CO_2 flux	0.33 ± 0.10	0.00 ± 0.17

[a] Units: heat fluxes, 10^{14} W; gas fluxes, 10^{14} mols a^{-1}. Fluxes are positive into the atmosphere.

Figure 6. Fluxes computed for various regions in the Atlantic and Antarctic Oceans from the 'composite' scenario. Heat fluxes are in units of 10^{14} W, O_2 and CO_2 fluxes are in units of 10^{14} mol a^{-1}.

showing these Southern hemisphere fluxes is only to illustrate qualitative differences in the patterns of O_2 and CO_2 exchange expected from the conveyor circulation in the Southern hemisphere.

We have assigned the fluxes associated with converting return–flow waters into NADW to the North Atlantic. Although we used hydrographic data spanning a wide range of latitudes (15 °S–15 °N) to characterize the return flow, we can, in fact, be somewhat more precise about where the boundary between the North and South Atlantic fluxes should be
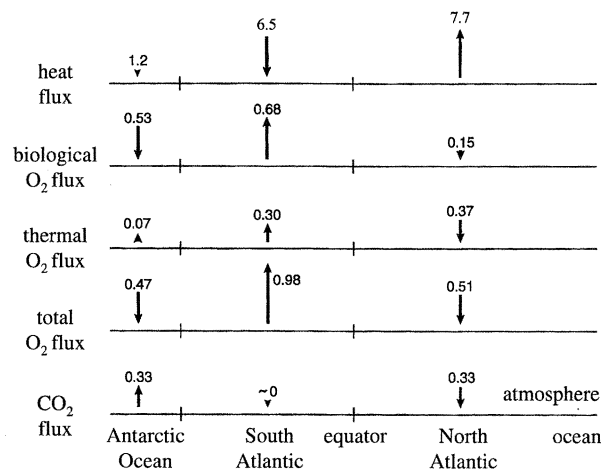
located. The key here is to note that, because our analysis neglects north–south transport associated with subtropical gyre circulation and with equatorial upwelling, the boundary needs to be drawn at the latitude band where the north–south transports caused by gyre and upwelling circulation are at their smallest.
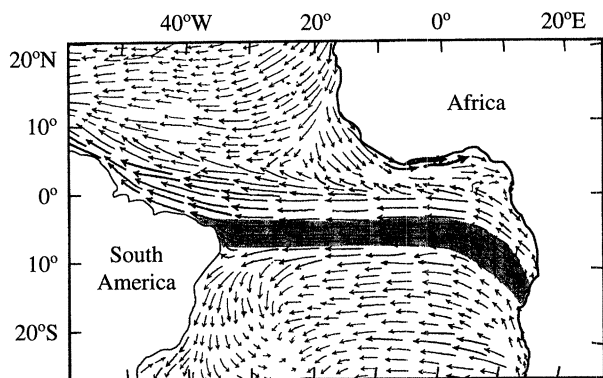
Figure 7. Map of the Atlantic surface currents in February, redrawn from Schott (1942). The grey area indicates the latitude band where the surface currents tend to run from Africa to South America.

We expect this condition to be achieved at the latitudes of intense equatorial upwelling, or equivalently, at the latitudes where the streamlines of the average surface currents run all the way from Africa to South America. From figure 7, therefore, we see that this boundary is probably best drawn somewhere between 0–10 °S. In contrast to the Southern hemisphere fluxes, the North Atlantic fluxes should approximate the total areally integrated exchange north of this boundary because we have chosen the boundary so as to minimize transports other than thermohaline transports.

According to figure 6, the total O_2 cycle can be largely explained on the basis of two subcycles: a biological cycle involving uptake of O_2 around Antarctica and release in the South Atlantic; and a thermal cycle involving O_2 release in the South Atlantic and uptake in the North Atlantic. The biological cycle is driven by photosynthetic uptake of nutrients along the conveyor's return path leading to the release of O_2 to the atmosphere and the export of organic carbon to the deep South Atlantic. The respiratory consumption of this organic carbon in the southward flowing plume of NADW releases nutrients and consumes O_2 from these waters. The O_2 undersaturation caused by this consumption results in O_2 uptake from the atmosphere when these waters upwell around Antarctica. The thermal cycle is driven by warming that occurs along the conveyor's return path in the South Atlantic and by cooling that occurs in the North Atlantic.

Although we have not attempted to divide the CO_2 fluxes into separate thermal and biological components, we can get a qualitative guide from a comparison with the O_2 fluxes. Thermal CO_2 fluxes have the same sign as thermal O_2 fluxes, while the dominant biological CO_2 fluxes driven by the formation and destruction of soft tissues have the opposite sign. This suggests that the CO_2 cycle can also be explained largely by two subcycles: a biological cycle involving CO_2 release in the Antarctic Ocean and uptake in the South Atlantic; and a thermal cycle involving CO_2 release in the South Atlantic and uptake in the North Atlantic. The sum of these two cycles yields the net exchanges shown in figure 6. Our finding that the net CO_2 flux is small in the South Atlantic requires that the biological and thermal effects on CO_2

exchange cancel each other out on average in this region. In the North Atlantic, the small biological O_2 flux is directed into the ocean so the biological CO_2 flux must be outward in this region. The fact that there is net CO_2 uptake requires that thermally driven CO_2 uptake more than compensates for the biological CO_2 release in the North Atlantic.

An important result from these calculations is that the exchanges of heat, total O_2, and 'biological' O_2 over the North Atlantic appear reasonably well constrained even though the waters contributing to the return flow are not yet well characterized. The key here is that θ, PO_4^*, and $PO_4^{(pref)}$ are all sufficiently well correlated with phosphate in the return-flow waters (figure 5), that, once the northward flux of phosphate is determined, the other fluxes are effectively determined as well. The correlations even hold reasonably well in the upper thermocline waters (12–24 °C), so the heat and O_2 fluxes would not change significantly even if we allowed upper thermocline water to contribute to the return flow. On the other hand, the phosphate constraint is not very helpful for constraining CO_2 fluxes because there is not even an approximate linear relationship between $\Delta\Sigma CO_2$ and PO_4 in the return-flow waters (figure 6). Excluding upper thermocline waters does indeed matter for CO_2 because $\Delta\Sigma CO_2$ has an extremum in these waters. Allowing this upper thermocline to contribute to the return flow would reduce the computed CO_2 uptake for the North Atlantic.

Our flux estimates for heat, CO_2, and O_2 are compared with other Atlantic studies in table 4. A previous study which examined both CO_2 and O_2 fluxes across 24 °N is that of Brewer *et al.* (1989), although comparison is difficult because their CO_2 fluxes are not corrected for anthropogenic CO_2, and because their O_2 transport is based on the flux of dissolved O_2, not on PO_4^*. To make a valid comparison for O_2 one would need to show that the flux of PO_4 was zero across the 24 °N transect.

Rintoul & Wunsch (1991) examined heat, O_2, and NO_3 fluxes across the 24 °N transect and found that the NO_3 flux (and thus presumably also the PO_4 flux) was not significantly different from zero although their O_2 flux is somewhat larger than that of Brewer *et al.* (1989). The Rintoul & Wunsch (1991) heat and O_2 fluxes at 24 °N are larger than the heat and O_2 fluxes reported here for the equatorial region, by factors of 1.69 and 1.80, respectively. Larger fluxes are expected at 24 °N than at the equator because the gyre circulation contributes to additional northward transport of heat and southward transport of O_2 at 24 °N. Our estimate of the heat transport across the equatorial region agrees quite well with previous estimates within rather wide error margins, as shown in table 4. It is satisfying that our value of $7.7 \pm 1.4 \times 10^{14}$ W lies midway between the apparently well-constrained estimates of $2.5 \pm 1.2 \times 10^{14}$ W at 32 °S (Rintoul 1991), and $12.2 \pm 3 \times 10^{14}$ W at 25 °N (Hall & Bryden 1982).

Our result for North Atlantic CO_2 flux agrees well with the result of Broecker & Peng (1992), if their result is scaled to a total flow of 13 *Sv*, as assumed here. Broecker & Peng (1992) base their calculation on the

Table 4. *Flux comparison*

	latitude	northward heat flux	southward CO$_2$ flux	southward O$_2$ flux
Hall & Bryden (1982)	25° N	12.2±3		
Wunsch (1984)	0°	2 to 10		
Hsiung (1985)[a]	0°	5.4		
Oberhuber (1988)[a]	0°	4		
Isemer *et al.* (1989)[b]				
unconstrained	0°	0±9		
constrained @ 24° N	0°	8 to 10		
Brewer *et al.* (1989)[c]	25° N		> 0.22	0.66
Rintoul & Wunsch (1991)	24° N	13±2		0.92±0.06
Rintoul (1991)	32° S	2.5±1.2		
Broecker & Peng (1992)				
unadjusted	∼ 0°		0.5	
adjusted[d]			0.32	
this study	0°	7.7±1.4	0.33±0.15	0.51±0.21

[a] The uncertainty in the Hsiung (1985) and Oberhuber (1988) estimates, although not reported, can be assumed to be comparable to the uncertainty in the unconstrained Isemer *et al.* (1989) calculation, which uses a similar method.
[b] Two estimates from Isemer *et al.* (1989) are listed. The unconstrained value corresponds to their result based on unconstrained bulk transport formulae. The constrained estimate corresponds to their result when the heat flux at 24° N is forced to lie between 10×10^{14}–12×10^{14} W.
[c] Following Broecker & Peng (1992) we interpret the Brewer *et al.* (1989) result as a lower bound to the preindustrial transport because their CO$_2$ transport is not corrected for excess anthropogenic CO$_2$ carried by the northward return flow.
[d] The adjusted number is the result Broecker & Peng (1992) would have obtained had they assumed a total conveyor flow of 13 *Sv* as opposed to 20 *Sv*.

difference between the $\Delta\Sigma CO_2$ of deep waters of northern and southern origin in the Atlantic, and as they point out, their calculation assumes that little CO$_2$ is exchanged along the conveyor's northward return path. Our results for the CO$_2$ exchange in the southern and equatorial Atlantic (table 3) support this assumption.

According to Schmitz & McCartney (1993), the northward return flow of the conveyor circulation is comprised of a mixture of 7 *Sv* 'surface' water (> 24 °C), 1 *Sv* 'thermocline' water (12–24 °C), and 5 *Sv* 'lower thermocline' water (7–12 °C). Our return-flow breakdown (table 2) is somewhat different. The maximum 'surface' flow compatible with the phosphate constraint is about 7 *Sv* ('intermediate water' scenario, table 2); but this requires that the remaining 6 *Sv* cross the equator as 6 °C intermediate water, not thermocline water. The phosphate constraint, therefore, seems to imply that either significantly less surface water is transported northward than proposed by Schmitz & McCartney (1993), or that a significant fraction of the return flow crosses the equator as intermediate water. Either way, our transports require a larger fraction of deeper water. Our best guess, based on the 'composite' scenario, would be that the return flow consists of approximately 4.8 *Sv* of surface water, 4.8 *Sv* of lower thermocline water, and 3.4 *Sv* of intermediate water. The need for a deep component to the return flow was previously noted by Broecker & Peng (1982, p. 346), who argued that the ^{14}C and nutrient content of NADW could only be explained if the source waters for NADW originated mostly at intermediate depths rather than at the surface.

While our flux calculations for the North Atlantic take account of variability in endmember composition and uncertainty in the phosphate budget, they do not account for errors that arise from oversimplification of flow patterns. What do our calculations really assume in this regard? Although it may appear that our calculations assume that the North Atlantic circulation involves nothing more or less than a single overturning cell, the calculations can, in fact, be justified on the basis of two less restrictive assumptions: (i) that a line can be drawn across the equatorial Atlantic, to the north of which, all water parcels at the surface eventually drift northward rather than southward, and (ii) north of this line all water parcels which are exposed to the surface eventually exit the North Atlantic as a component of NADW. Thus our North Atlantic flux calculations should be quantitatively accurate as long as there are no significant pathways for surface water to leave the North Atlantic other than as NADW. As far as we are aware, the only pathway of this sort which has been clearly identified is via water flowing out of the Mediterranean Sea, some of which intermixes with NADW and migrates southward (Reid 1994). The flows involved here are small, however.

In any case, an evaluation of the magnitude of the errors arising from the oversimplification of the flow patterns will require a closer examination of north–south mass transports, especially in the tropics. Our calculations emphasize the value of the nutrient distributions for constraining large-scale flows in the Atlantic, especially in the equatorial region where computing mass transports via the standard physical oceanographic approximations is problematic.

REFERENCES

Bainbridge, A.E. 1981 *GEOSECS Atlantic Ocean Expedition hydrographic data VI*. Washington DC: NSF.

Björk, G. 1990 The vertical distribution of nutrients and oxygen 18 in the upper Arctic ocean. *J. geophys. Res.* **95**, 16025–16036.

Brewer, P.G., Goyet, C. & Dyrssen, D. 1989 Carbon dioxide transport by ocean currents at 25° N latitude in the Atlantic Ocean. *Science, Wash.* **246**, 477–479.

Broecker, W.S. 1991 The great ocean conveyor. *Oceanography* **4**, 79–89.

Broecker, W.S. & Peng, T.-H. 1982 *Tracers in the sea*. Palisades, New York: Lamont-Doherty Geological Observatory.

Broecker, W.S. & Peng, T.-H. 1992 Interhemispheric transport of carbon dioxide by ocean circulation. *Nature, Lond.* **356**, 587–589.

Broecker, W.S., Virgilio, A. & Peng, T.-H. 1991 Radiocarbon age of waters in the deep Atlantic revisited. *Geophys. Res. Let.* **18**, 1–3.

Broecker, W.S. & Peng, T.-H. 1993 Interhemispheric transport of carbon through the ocean. In *The global carbon cycle, proceedings of the NATO Advanced Study Institute on the contemporary global carbon cycle* (ed. M. Heimann), pp. 551–570. Berlin: Springer Verlag.

Coachman, L. K. & Aagaard, K. 1988 Transports through Bering strait: annual and interannual variability. *J.geophys.Res.* **93**, 15535–15539.

Codispoti, L.A. & Owens, T.G. 1975 Nutrient transports through Lancaster Sound in relation to the Arctic Ocean's reactive silicate budget and the outflow of Bering Strait waters. *Limnol. Oceanogr.* **20**, 115–119.

Gordon, A.L. 1985 Indian-Atlantic transfer of thermocline water at the Argulhas retroreflection. *Science, Wash.* **227**, 1030–1033.

Hall, M.M. & Bryden, H.L. 1992 Direct estimates and mechanisms of ocean heat transport. *Deep Sea Res.* **29**, 339–359.

Hsiung, J. 1985 Estimates of global oceanic meridional heat transport. *J. phys. Oc.* **15**, 1405–1413.

Isemer, H.-J., Willebrand, J. & Hasse, L. 1989 Fine adjustment of large scale air–sea energy flux parameterizations by direct estimates of ocean heat transport. *J. Climate* **2**, 1173–1184.

Keeling, C.D., Piper, S.C. & Heimann, M. 1989 A three-dimensional model of atmospheric CO_2 transport based on observed winds: 4. mean annual gradients and interannual variations. In *Aspects of climate variability in the Pacific and Western Americas* (ed. D.H. Peterson), pp. 305–363. Washington, D.C.: American Geophysical Union.

Keeling, R.F. & Shertz, S.R. 1992 Seasonal and interannual variations in atmospheric oxygen and implications for the global carbon cycle. *Nature, Lond.* **358**, 723–727.

Keeling, R.F. Najjar, R.G., Bender, M.L. & Tans, P.P. 1993 What atmospheric oxygen measurements can tell us about the global carbon cycle. *Global biogeochem. Cycles* **7**, 37–67.

Meybeck, M. 1982 Carbon, nitrogen, and phosphorous transport by world rivers. *Am. J. Sci.* **282**, 401–450.

Oberhuber, J.M. 1988 *Report No. 15, An atlas based on the COADS set: the budgets of heat, buoyancy and turbulent kinetic energy at the surface of the global ocean*, pp. 1–20. Hamburg: Max-Planck-Institut für Meteorologie.

Peng, T.-H. & Broecker, W.S. 1987 C/P ratios in marine detritus. *Global biogeochem. Cycles.* **1**, 155–161.

Redfield, A.B., B.H. Ketchum, B.H. & Richards, F.A. 1963 The influence of organisms on the composition of seawater. In *The sea*, vol. 2 (ed. by M.N. Hill), pp. 26–77. New York: Wiley Interscience.

Reid, J. L. 1994 On the total geostrophic circulation of the North Atlantic Ocean: flow patterns, tracers, and transports. *Prog. Oceanog.* **33**, 1–92.

Rintoul, S.R. 1991 South Atlantic interbasin exchange. *J. geophys. Res.* **96**, 2675–2692.

Rintoul, S.R., Wunsch, C. 1991 Mass, heat, oxygen and nutrient fluxes and budgets in the North Atlantic ocean. *Deep Sea Res.* **38** (Suppl. 1), S355–S377.

Schmitz, W.J. & McCartney, M.S. 1993 On the North Atlantic circulation. *Rev. Geophys.* **31**, 29–49.

Schmitz, W.J. Jr & Richardson, P.L. 1991 On the sources of the Florida Current. *Deep Sea Res.* **38** (Suppl. 1), S379–S409.

Schott, G. 1942 *Geographie des Atlantischen Ozeans*. Hamburg: C. Boysen.

Scripps Institution of Oceanography 1986 *Transient Tracers in the Ocean, North Atlantic Study, Shipboard Physical and Chemical Data Report*. San Diego: Scripps Institution of Oceanography.

Scripps Institution of Oceanography, 1988–1989 *South Atlantic Ventilation Experiment, Preliminary Shipboard Chemical and Physical Data Report*. San Diego: Scripps Institution of Oceanography.

Takahashi, T., Broecker. W.S. & Langer, S. 1985 Redfield ratio based on chemical data from isopycnal surfaces. *J. geophys. Res.* **90**, 6907–6924.

Tans, P.P., Fung, I.Y. & Takahashi, T. 1990 Observational constraints on the atmospheric CO_2 budget. *Science, Wash.* **247**, 1431–1438.

Wunsch, C. 1984 An eclectic Atlantic Ocean circulation model. Part 1: The meridional flux of heat. *J. phys. Oc.* **14**, 1712–1733.